Steel and Composite Structures, *Vol. 19, No. 6 (2015) 1355-1367*
DOI: http://dx.doi.org/10.12989/scs.2015.19.6.1355

Experiments on locally dented conical shells under axial compression

Tohid Ghanbari Ghazijahani*[a], Hui Jiao [b] and Damien Holloway [c]

School of Engineering and ICT, *University of Tasmania*, *Sandy Bay Campus*, *Hobart*, *TAS 7001*, *Australia*

(*Received February 26, 2015, Revised May 03, 2015, Accepted May 28, 2015*)

Abstract. Steel conical shells have long been used in various parts of different structures. Sensitivity to the initial geometrical imperfection has been one of the most significant issues on the stability of these structures, which has made them highly vulnerable to the buckling. Most attention has been devoted to structures under normal fabrication related imperfections. Notwithstanding, the challenges of large local imperfections – presented herein as dent-shaped imperfections – have not been a focus yet for these structures. This study aims to provide experimental data on the effect of such imperfections on the buckling capacity of these shells under axial compression. The results show changes in the buckling mode and the capacity for such damaged thin specimens as is outlined in this paper, with an average overall capacity reduction of 11%.

Keywords: conical steel shells; buckling; axial loading; dent; local imperfection

1. Introduction

Steel conical shells are commonly seen in different elements of engineering structures. These structures are sometimes used as transition components known as *reducers* to connect two cylindrical shells with different radiuses. Much research can be found on the stability of such structures. El-Sobky and Singace studied compressed frusta (truncated cones) in an experimental study (El-Sobky and Singace 1999). The elastic stress profiles of specimens with different boundary conditions were investigated in this study. Buckling of thin conical frusta under axial loads was studied by Gupta *et al*., wherein rolling and stationary plastic hinges were seen as two different failure modes (Gupta *et al*. 2006). Axisymmetric axial crushing of thin frusta was studied by Gupta and Abbas in a theoretical research (Gupta and Abbas 2000). The size of folded area and the variation of crushing load are theoretically found in this paper. An experimental study on the deformation modes of domes and large-angled truncated cones subjected to axial loading was studied by Prasad and Gupta (Prasad and Gupta 2005).

Over the past few years the buckling of conical shells with different geometries was discussed by (Błachut 2011, Ifayefunmi 2011, Sofiyev 2011, Zhao and Liew 2011, Błachut 2012, Błachut *et*

*[a] Corresponding author, Ph.D. Student, E-mail: tohid.ghanbari@utas.edu.au; tohidghanbari@gmail.com
[b] Ph.D., E-mail: hui.jiao@utas.edu.au
[c] Ph.D., E-mail: damien.holloway@utas.edu.au

 ISSN: 1229-9367 (Print), 1598-6233 (Online)

al. 2013) and different aspects of stability problems in these structures were examined. The collapse mode of metallic frusta with varying wall thickness was studied by Gupta (2008). Different deformed profiles with different values of compression were obtained in this research. Sensitivity of these structures with different imperfections was studied by Showkati and his co-authors in several studies (Golzan and Showkati 2008, Ghanbari Ghazijahani and Showkati 2011, Maali *et al*. 2012, Ghanbari Ghazijahani and Showkati 2013a, b, Ghanbari Ghazijahani and Zirakian 2014). It was found that the sensitivity of conical shells to imperfections was less significant under different loadings such as external pressure than to axial load. Stability of specimens with different diameter to thickness ratios (D/t) was reported in these references.

It should be mentioned that most of the references available in the literature have presented the buckling behavior of such structures under normal fabrication-related imperfections on the body of these structures. These imperfections are often in the form of global out-of-roundness of different sections or randomly distributed projections and/or depressions resulted from rolling or machining shortcomings throughout the fabrication. These imperfections are mostly of small-amplitude and depth which make these structures appear visually to have perfect geometry. However, Ghanbari Ghazijahani *et al*. recently conducted two experimental studies on thin cylindrical specimens, which were geometrically similar to the specimens of the present study and two researches on steel dented tubes (Ghanbari Ghazijahani *et al*. 2014a, b). It appeared that dent imperfection have a moderate effect on the failure mode and the capacity of very thin structures, but considerable effect on the capacity of thicker tube specimens (Ghanbari Ghazijahani *et al*. 2015a, c).

Apart from the mentioned studies there is an absence of studies on large imperfections (e.g., dent/gouge-shaped imperfections) in the literature, in particular for conical shells. To this end, dented thin truncated cones were studied in this research under axial loading, and the buckling capacity and the failure modes were thoroughly investigated.

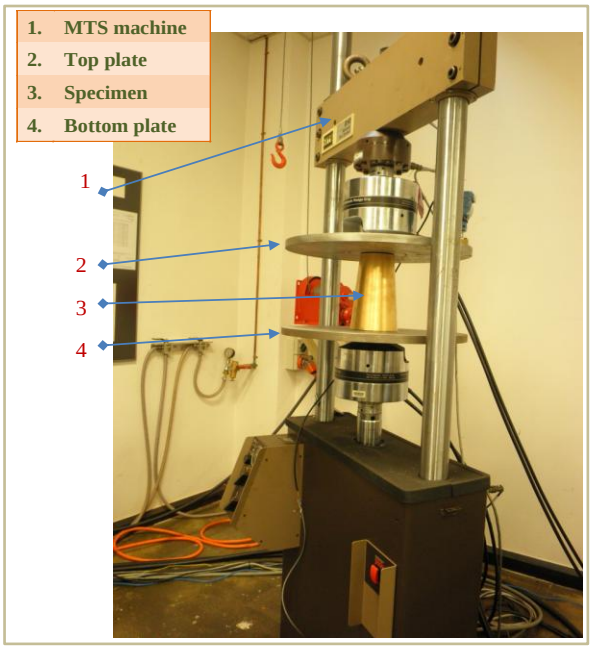

Fig. 1 Overall view of the test rig

Fig. 2 Specimens and dent imperfections

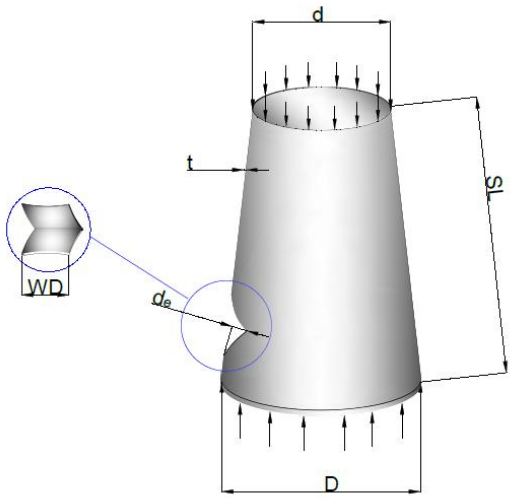

Fig. 3 Geometry of the specimens and dent imperfection

Table 1 Geometry of the specimens

Specimen	t (mm)	d (mm)	D (mm)	D_m/t	SL/D_m	α	Height (mm)
CONE.1–9	0.2	92.7	113.2	566	1.1	10°	118.2

Note: The mean value of the diameter: $D_m = (D + d)/2$ (symbols defined in Fig. 3)

2. Experimental set-up

Specimens were all company-made mild steel with a mild taper of the geometry (see Table 1 for details). Both ends of the specimens were machined such that the edges were in contact with the end plates before the tests. Specimens were labelled as CONE.1–9. The first three specimens were intact ones (undented); CONE.4, CONE.7 and CONE.9 were indented 30 mm from the top edge, CONE.5 and CONE.6 were indented 30 mm from the bottom edge and a dent was located at 15 mm from the top for CONE.8 and all dents were in the circumferential direction (see Table 2 for details of the dent imperfections).

The authors used a *MTS-810 Material Testing System* in order to apply the compression load to the specimens. This machine was calibrated by *ACS* (*Australian Calibrating Services*) to ensure the accuracy of the function during the experimentations. The specimens were placed between two plates. These plates were gripped by jaws of the machine and, meticulous attention was paid to align the plates. Overall view of the test rig and the geometry of specimens are presented in Figs.

Table 2 Major geometric features of the dented area for each specimen

Specimen	d_e (mm)	WD (mm)	t/WD	t/d_e	d_e/WD
CONE.1	–	–	–	–	–
CONE.2	–	–	–	–	–
CONE.3	–	–	–	–	–
CONE.4	0.8	25	0.008	0.25	0.03
CONE.5	1	23	0.009	0.20	0.04
CONE.6	1.9	42	0.005	0.11	0.05
CONE.7	2.8	43	0.005	0.07	0.07
CONE.8	4	47	0.004	0.05	0.09
CONE.9	4	50	0.004	0.05	0.08

1-3. In Fig. 3, d and D are the diameters of small and large ends, SL is the slant length, t is the thickness d_e and W_d are the depths and the width of the dented area respectively.

The desired dent zone was accurately marked at a predetermined distance from the top or bottom end. Dent imperfections were made by means of a hard metal indenter shown in Fig. 4. The indenter was circle-edged through which a controllable dent was made through a steady and gentle hand movement of the indenter over the surface of the shells. Tensile coupon test was conducted on a few specimens shaped to AS 1391-2007 specifications to obtain the material properties. The *Young's modulus* and *Poisson's ratio* were 200 GPa and 0.3 respectively.

In this set of experiments the displacement control method was adopted, in which constant but

Fig. 4 Indenter (left), and gauge to measure the geometry of the dented area (right)

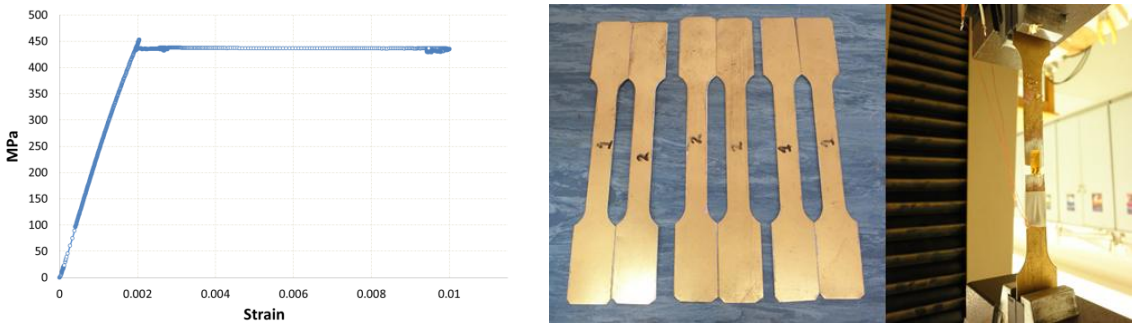

Fig. 5 Tensile coupon test: stress strain curve (left), specimens and failure (right)

slow rate of loading speed was employed throughout the tests to reach a quasi-static testing. Whilst loading, a camera was recording the whole experiments in order to later review the buckling progress. Axial shortening of the specimens and loading magnitudes were recorded by a data acquisition system connected to the MTS machine and an installed LabVIEW, 2012 program.

3. Test results

3.1 Observations, failure mode

CONE.1–3, intact shells:

As seen in Fig. 6, two stages of deformations were observed for the intact specimens. A ring-shaped deformation, known as elephant foot buckling mode, was typically detected at the top end of all intact cones. This mode exhibited an outward deformation at around 4 mm from the top edge of the specimens. As buckling progressed diamond-shaped buckling lobes were initiated one after another and the elephant foot transitioned into another mode known as diamond mode (Fig. 7). Buckling in this mode occurred initially in one tier and as the load increased the diamonds became severely distorted as the specimen gradually crushed. As a result a considerable length of the top region of the specimens was axially crumpled into tiers. The bottom end, on the other hand, was not significantly affected by any deformation, although the edge section was no longer perfect in terms of roundness and a few small deformational waves were seen.

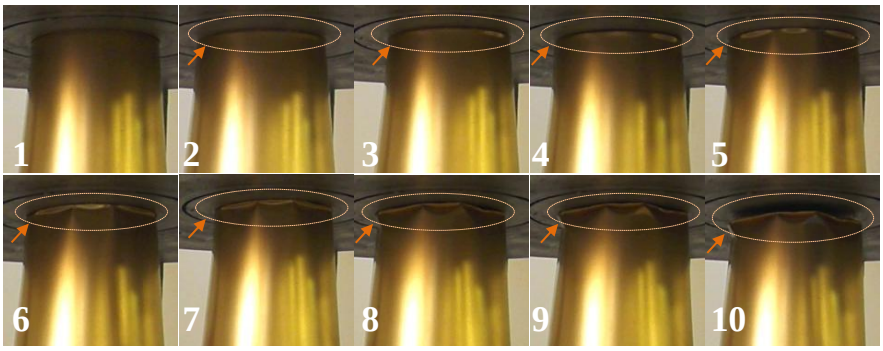

Fig. 6 Initiation of *elephant foot* mode of bucking and transition into *diamond mode* in an intact specimen

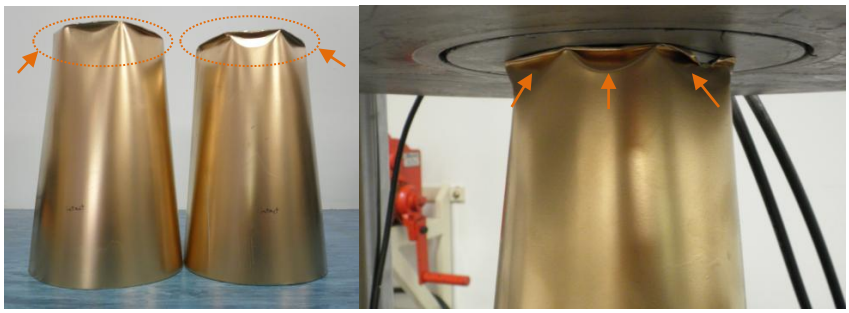

Fig. 7 Diamond mode of failure

CONE.4–9, dented specimens:

Buckling was initiated in the dented specimens both at the top end and simultaneously in the vicinity of the dented area. The ring-shaped deformation was formed in the dented specimens in a similar way to the intact ones. However, deepening of the dent and extension of the amplitude of the dented zone was accompanied by the elephant foot mode of buckling at the top end.

As loading progressed in specimens with smaller dents the dent deformed in curved shapes around the dented zone, growing towards the top end. This continued until the dented zone subsequently reached the yield-lines of the ring-shaped deformation and eventually combined with the diamond waves.

On the other hand for the specimens with larger dents the deformations developed mostly horizontally along the dent, although the top region of the dent touched the diamond-shaped buckling waves. Buckling progress of two dented specimens is seen in Figs. 8 and 9. Schematic

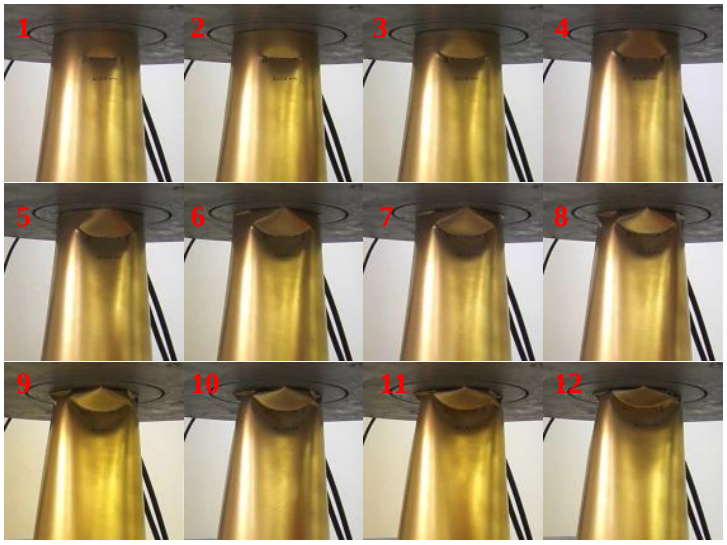

Fig. 8 Buckling progress in specimen CONE.4

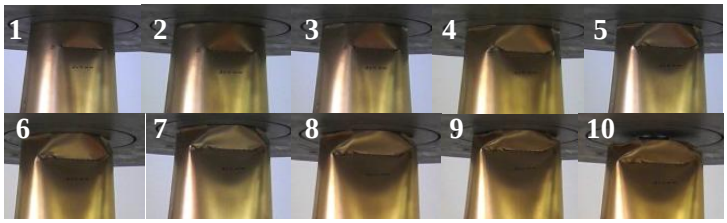

Fig. 9 Buckling progress in specimen CONE.9

Fig. 10 Schematic layout of the buckling progress in a dented specimen

Fig. 11 Crumpled failure in the top end of different specimens

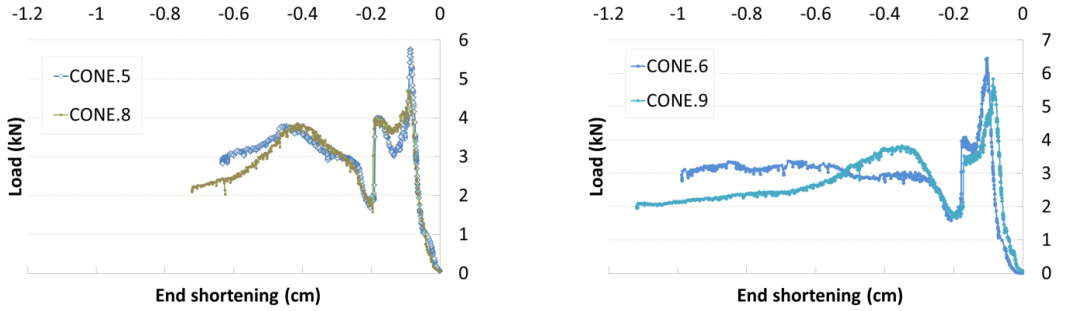

Fig. 12 Axial load versus end shortening plots for specimen CONE.5, CONE6, CONE.8 and CONE.9

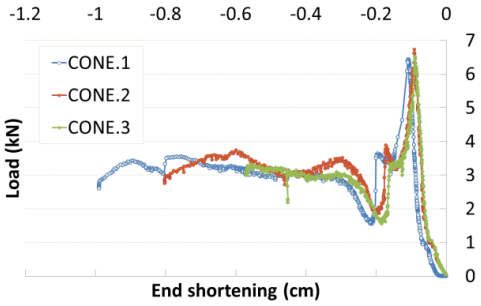

Fig. 13 Load–end shortening for the intact specimens

illustrations of the buckling initiation and development are presented in Fig. 10. It was interesting that the final shape of the end edge was chiefly hexagonal after the tests (see extreme left view in Fig. 11).

3.2 Load displacement curves

Fig. 12 plots axial load versus end shortening of the specimens CONE.5, CONE6, CONE.8 and CONE.9, which show typical load displacement trends for these shell structures. Fig. 13 shows the same curves for three different intact specimens. Bifurcation of displacement can be observed in these curves, in which the load plunged steeply after the peak load was obtained. This bifurcation was followed by two fluctuation waves in the load-displacement curve during the post-buckling stage. It is quite evident that the curves were more stable for the intact specimens than for the dented ones during post-buckling, i.e., the dented specimen curves experienced deeper fluctuations. It is noteworthy that the load-displacement curve for the cylindrical specimens in Ref. (Ghanbari

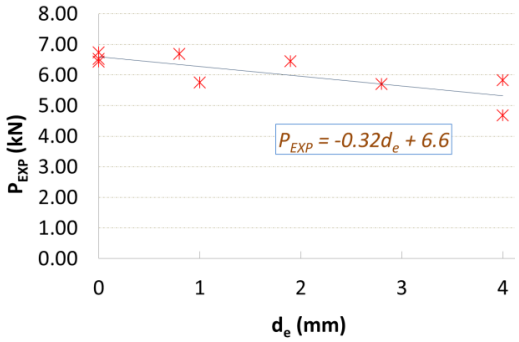

Fig. 14 Load versus the depth of the dent

Ghazijahani *et al*. 2014a) decreased and/or was steady, whereas for the present conical shells a rise-and-fall trend was obtained after initial buckling.

4. Buckling capacity of the frusta

To ensure that the capacity of the intact specimen, which is deemed as a control specimen, was accurately obtained, three replicates were tested to failure. Fig. 14 shows the buckling capacity of the present conical shells both for the intact and the dented models. An average reduction of 11% due to the dents was obtained, among which CONE.8 accounted for the maximum decrease. This is believed to be due to the combined effect of the depth of the dent and the proximity to the top edge. Dented zones in the vicinity of the bottom end had rather milder effects on the buckling capacity than the dents located near the top end. This can be attributed to the fact that the top end was indeed more susceptible to buckling under axial compression, as reported in the previous references outlined in the introduction section.

Overall, the decreasing trend shown in Fig. 14 indicates a relatively moderate reduction in the buckling capacity for these shells. It should be mentioned that, as discussed in (Ghanbari Ghazijahani *et al*. 2014a, b), the ultimate capacity of the dented shells can be affected by an interrelation of the geometrical irregularity on the one hand, and the material change on the other hand. The material of these thin structures can be strongly affected by the local loads throughout the indentation process, which can lead to the strain hardening of the material in the dented area. This can generally cause nonlinear effects in the material. As a consequence, the total stiffness of the dented zone will change relative to the intact zone, which in some cases may cause some local strengthening. Showkati *et al*. in Refs. (Maali *et al*. 2012, Fatemi *et al*. 2013, Niloufari *et al*. 2014) and Ghanbari Ghazijahani *et al*. in Refs. (Ghanbari Ghazijahani *et al*. 2014a, b, Ghanbari Ghazijahani *et al*. 2015b) have already observed this in some of their specimens during mentioned studies.

5. Comparison with previous studies

5.1 Comparison of the results with the theoretical equations

In this section, the results of the current study are evaluated against the available theoretical

estimations. Seide proposed Eq. (1) for prediction of the critical buckling load of the truncated conical shells (Seide 1956). In this equation, γ equals 0.33 for cones with $10° < \alpha < 75°$ in which α denotes the semi-vertex angle of the cones, E is *Young's modulus*, t is the thickness of shells and μ is the *Poisson's ratio*.

$$P_{cr} = \gamma \frac{2\pi E t^2 \cos^2 \alpha}{\sqrt{3(1-\mu^2)}} \tag{1}$$

Additionally, Lackman and Penzien proposed an equation as Eq. (2) for the buckling load estimation of conical shells (Lackman and Penzien 1960). In this equation, "C" is a correction factor as a function of $R/(t\cos\alpha)$ which can be obtained using a graph in the mentioned reference.

$$P_{cr} = 2\pi C E t^2 \cos^2 \alpha \tag{2}$$

Fig. 15 shows the ratio of the buckling load derived from this experimental study over the theoretical values. Good consistency was obtained between the test results and the results of Eq. (1) where the experimental buckling load for the intact specimen was 70% of the theoretical value. However, considering Eq. (2) only around half of the theoretical magnitude was obtained through the tests. This indicates that, Eq. (1) can reasonably predict the approximate buckling load of the specimens with similar geometries. Despite this, Eq. (1) still overestimates the capacity, which is normal and attributed to the geometrical imperfections existing both in the specimens and the testing apparatus (Ghanbari Ghazijahani and Showkati 2013a). Additionally, the results of damaged cylindrical shells under compression for recent research of Ghanbari Ghazijahani *et al.* were presented for two types of specimens with different D/t ratios, i.e., LCC and SCC (Ghanbari

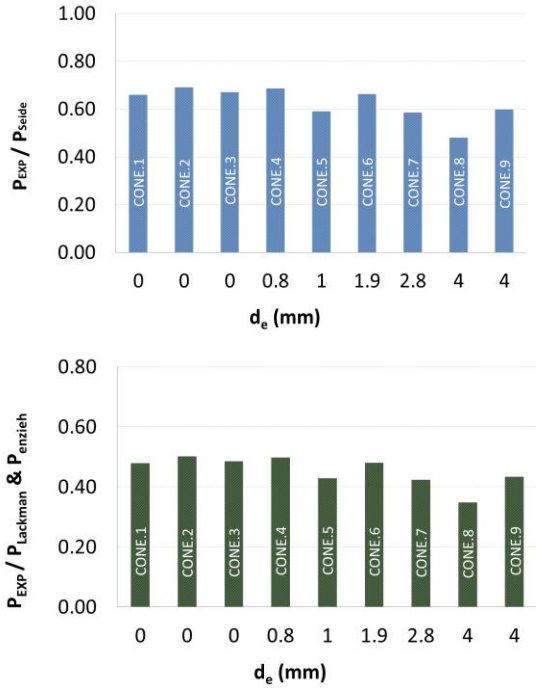

Fig. 15 Comparison of the results with the previous studies

Ghazijahani *et al*. 2014a). *D* and *t* were the nominal diameter and thickness of cylindrical shells. It clearly appears that the effect of the dent imperfection was quite similar to the conical shells under compression and the detrimental effect of the dent imperfection was mild in both studies.

5.2 Large imperfections in the literature

The magnitudes of the allowed imperfections have been reported in a few codes and standards. Fig. 16 shows the geometry of the dimple measured in EN 1993-1-6 (EN1993 2007). Limit bounds

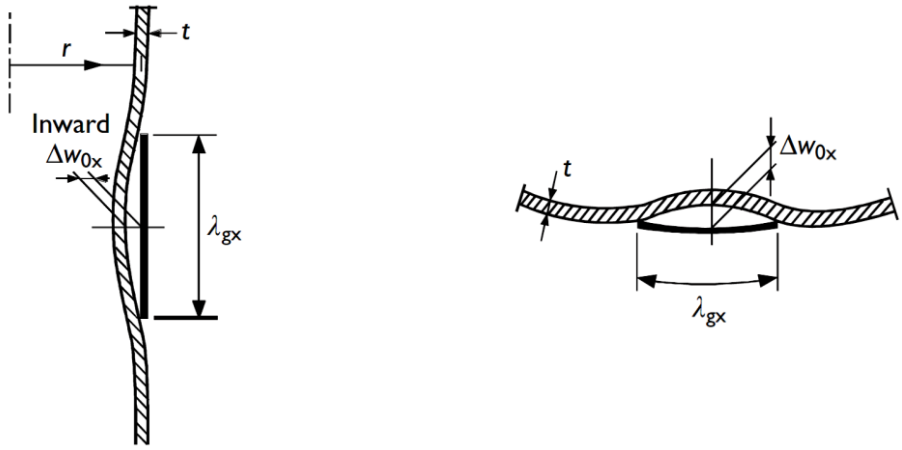

(a) (b)

Fig. 16 Dimple geometry measured by ENV 1993-1-6 (1999): (a) on a meridian; and (b) circumferential direction

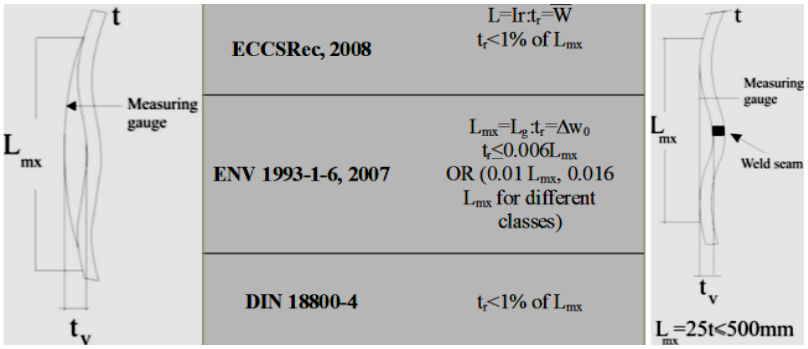

Fig. 17 ECCS, EN and DIN standards' tolerated values (Fatemi *et al*. 2013)

Table 3 ECCS, EN and DIN standards' tolerated values (Fatemi *et al*. 2013)

Tolerance quality class	Quality description	$U_{0,\,max}$	Q
Class A	Excellent	0.006	40
Class B	High	0.01	25
Class C	Normal	0.016	16

of geometric imperfections are also seen in Fig. 17, wherein the tolerated imperfections in ECCS, EN and DIN codes are presented (ECCS 2008, DIN 1990, EN1993 2007). Eq. (3) presents the allowable depth of the imperfection (Δw_x), where Q denotes a fabrication quality parameter which is obtained from Table 3. Additionally, U_{0x} in Eq. (4) shows the dimensionless parameter of the imperfections which is tolerated using the values listed in Table 3 considering different qualities of fabrication defined for shell structures (Teng and Rotter 2006). Note that l_r, l_g and l_{mx} are defined as longitudinal imperfections which are made in a hoop direction.

$$\Delta w_x = \frac{t}{Q}\sqrt{r/t} \tag{3}$$

$$U_{0x} = \frac{\Delta w_{0x}}{\lambda_{gx}} \tag{4}$$

The consensus view regarding the imperfection sensitivity of shell structures is that only the geometric imperfections whose geometry is less than the tolerated magnitudes in the codes are allowed in structural elements. Nevertheless, the recent experimental works conducted on large locally imperfect thin shells subject to different load cases propounds a view that despite large local irregularities of the geometry of the imperfections, local imperfections in some cases may not have significant effects on the capacity – as much as would have been expected – relative to the normal fabrication-related imperfections. Experimental findings lend support to this claim as can be found in Refs. (Maali *et al*. 2012, Fatemi *et al*. 2013, Ghanbari Ghazijahani *et al*. 2014b, Niloufari *et al*. 2014). In fact, this view is grounded on the assumption that for thin shells the rigidity of the material at the dented area, i.e., severely imperfect zone, can be largely affected by local loading applied during the indentation process which, as discussed, may lead to a sort of strengthening effect. Overall, there seem to be an interrelation between the geometrical irregularity and the material properties of the dented zone. The former, results in an adverse effect on the capacity, whereas the latter appears to have a positive effect. Clearly, further research into this problem is still required in order to extend this knowledge before drawing a definitive conclusion.

6. Conclusions

This research investigated the influence of large imperfections on the buckling and failure behavior, and the capacity of the truncated conical shells subjected to axial compression. Intact and imperfect thin shells with simply supported boundary conditions were tested to failure. The key findings of this study can be summarized as:

(i) For intact specimens two stages of deformations were observed. A ring-shaped deformation, known as elephant foot buckling mode, was typically detected at the top end of all intact cones. Following that, diamond-shaped buckling lobes were initiated one after another such that the *elephant foot* transitioned into another buckling mode, i.e., *diamond mode* of buckling.

(ii) For the dented specimens, buckling was initiated simultaneously at the top end and in the vicinity of the dented area.

(iii) Bifurcation of displacement was observed, in which the load plunged steeply after the peak load was obtained. This bifurcation was followed by two fluctuation waves respectively in load-displacement curve during the post-buckling stage.

(iv) The dented specimens exhibited a relatively moderate reduction in the buckling capacity. An average decrease of 11% was obtained compared with the intact speciemens, in which CONE.8 accounted for the maximum decrease.
(v) Dented zones in the vicinity of the bottom end had rather milder effects on the buckling capacity than the dents located near the top end.
(vi) Good consistency was obtained between the test results and the results of Eq. (1). The experimental buckling load for the intact specimen was 70% of the theoretical value.
(vii) There seems to be an interrelation between the geometrical irregularity and the material properties of the dented zone. The former results in an adverse effect on the capacity whereas the latter appears to have a positive effect. Yet, further research into this problem is still required in order to extend this knowledge before drawing a definitive conclusion.

Acknowledgments

The authors wish to greatly acknowledge *University of Tasmania* for the supports, workshop technicians especially Mr. Peter Seward, for their assistance during the experimentation.

References

Błachut, J. (2011), "On elastic–plastic buckling of cones", *Thin-Wall. Struct.*, **49**(1), 45-52.
Błachut, J. (2012), "Interactive plastic buckling of cones subjected to axial compression and external pressure", *Ocean Eng.*, **48**, 10-16.
Błachut, J., Muc, A. and Ryś, J. (2013), "Plastic buckling of cones subjected to axial compression and external pressure", *J. Press. Vessel Technol.*, **135**(1), 011205.
DIN 18800 (1990), Stahlbauten.Teil 4: Stabilitätsfalle, Schalenbeulen.
ECCS EDR5 (2008), European Recommendations for steel construction, Buckling of shells, (5th Ed.), In: Rotter, J.M., Schmidt, H., Editors, European convention for constructional steelwork, Brussels, Belgium, 384 p.
El-Sobky, H. and Singace, A. (1999), "An experiment on elastically compressed frusta", *Thin-Wall. Struct.*, **33**(4), 231-244.
EN1993-1-6 (2007), Eurocode 3: Design of steel structures, Part 1.6: General rules—Strength and stability of shell structures, Eurocode 3 Part 1.6, CEN, Brussels, Belgium.
Fatemi, S.M., Showkati, H. and Maali, M. (2013), "Experiments on imperfect cylindrical shells under uniform external pressure", *Thin-Wall. Struct.*, **65**, 14-25.
Ghazijahani, T.G. and Showkati, H. (2011), "Experiments on conical shell reducers under uniform external pressure", *J. Construct. Steel Res.*, **67**(10), 1506-1515.
Ghanbari Ghazijahani, T. and Showkati, H. (2013a), "Experiments on cylindrical shells under pure bending and external pressure", *J. Construct. Steel Res.*, **88**, 109-122.
Ghanbari Ghazijahani, T. and Showkati, H. (2013b), "Locally imperfect conical shells under uniform external pressure", *Strength Mater.*, **45**(3), 369-377.
Ghanbari Ghazijahani, T. and Zirakian, T. (2014), "Determination of buckling loads of conical shells using extrapolation techniques", *Thin-Wall. Struct.*, **74**, 292-299.
Ghanbari Ghazijahani, T., Jiao, H. and Holloway, D. (2014a), "Experimental study on damaged cylindrical shells under compression", *Thin-Wall. Struct.*, **80**, 13-21.
Ghanbari Ghazijahani, T., Jiao, H. and Holloway, D. (2014b), "Experiments on dented cylindrical shells under peripheral pressure", *Thin-Wall. Struct.*, **84**, 50-58.
Ghanbari Ghazijahani, T., Jiao, H. and Holloway, D. (2015a), "Fatigue tests of damaged tubes under flexural loading", *Steel Compos. Struct., Int. J.*, **19**(1), 223-236.

Ghanbari Ghazijahani, T., Jiao, H. and Holloway, D. (2015b), "Longitudinally stiffened corrugated cylindrical shells under uniform external pressure", *J. Construct. Steel Res.*, **110**, 191-199.
Ghanbari Ghazijahani, T., Jiao, H. and Holloway, D. (2015c), "Plastic buckling of dented steel circular tubes under axial compression: An experimental study", *Thin-Wall. Struct.*, **92**, 48-54.
Golzan, B. and Showkati, H. (2008), "Buckling of thin-walled conical shells under uniform external pressure", *Thin-Wall. Struct.*, **46**(5), 516-529.
Gupta, P. (2008), "A study on mode of collapse of varying wall thickness metallic frusta subjected to axial compression", *Thin-Wall. Struct.*, **46**(5), 561-571.
Gupta, N. and Abbas, H. (2000), "Axisymmetric axial crushing of thin frusta", *Thin-Wall. Struct.*, **36**(3), 169-179.
Gupta, N., Sheriff, N.M. and Velmurugan, R. (2006), "A study on buckling of thin conical frusta under axial loads", *Thin-Wall. Struct.*, **44**(9), 986-996.
Ifayefunmi, O.F. (2011), *Combined Stability of Conical Shells*, University of Liverpool, UK.
Lackman, L. and Penzien, J. (1960), "Buckling of circular cones under axial compression", *J. Appl. Mech.*, **27**(3), 458-460.
Maali, M., Showkati, H. and Mahdi Fatemi, S. (2012), "Investigation of the buckling behavior of conical shells under weld-induced imperfections", *Thin-Wall. Struct.*, **57**, 13-24.
Niloufari, A., Showkati, H., Maali, M. and Mahdi Fatemi, S. (2014), "Experimental investigation on the effect of geometric imperfections on the buckling and post-buckling behavior of steel tanks under hydrostatic pressure", *Thin-Wall. Struct.*, **74**, 59-69.
Prasad, G. and Gupta, N. (2005), "An experimental study of deformation modes of domes and large-angled frusta at different rates of compression", *Int. J. Impact Eng.*, **32**(1), 400-415.
Seide, P. (1956), "Axisymmetric buckling of circular cones under axial compression", *J. Appl. Mech.*, **23**(4), 625-628.
Sofiyev, A. (2011), "Influence of the initial imperfection on the non-linear buckling response of FGM truncated conical shells", *Int. J. Mech. Sci.*, **53**(9), 753-761.
Teng, J.-G. and Rotter, J.M. (2006), *Buckling of Thin Metal Shells*, CRC Press.
Zhao, X. and Liew, K.M. (2011), "An element-free analysis of mechanical and thermal buckling of functionally graded conical shell panels", *Int. J. Numer. Method. Eng.*, **86**(3), 269-285.

CC